Environmental Science and Pollution Research (2021) 28:5149–5157
https://doi.org/10.1007/s11356-020-10859-0

RESEARCH ARTICLE

Efficient removal of cadmium ions from water by adsorption on a magnetic carbon aerogel

Yingchao Li[1] · Mengqi Zhou[1] · Geoffrey I. N. Waterhouse[1,2] · Jianchao Sun[3] · Weijie Shi[1] · Shiyun Ai[1]

Received: 28 May 2020 / Accepted: 14 September 2020 / Published online: 21 September 2020

Abstract

Carbon aerogels are attracting much attention as adsorbents due to their high specific surface and large accessible pores. Herein, we describe a successful synthesis of a magnetic carbon aerogel (MCA) using sodium alginate (SA) as the main carbon source, gelatin (G) as a cross-linking agent and secondary carbon source, and Fe_3O_4 nanoparticles as the magnetic component. A simple pyrolysis treatment at 550 °C under N_2 transformed a Fe_3O_4/SA/G hydrogel precursor into the MCA. The obtained magnetic carbon aerogel possessed a high specific surface area (145.7 m^2/g), a hierarchically porous structure, and an abundance of surface hydroxyl (–OH) and carboxyl (–COOH) groups, resulting in outstanding sorption properties for aqueous Cd(II) (an adsorption capacity of 143.88 mg/Lmg/g). The mechanism of Cd(II) adsorption by the MCA was investigated, with the results obtained suggesting that the MCA removed cadmium ions from water by both electrostatic adsorption and complexation. Since the MCAs contained Fe_3O_4 nanoparticles, they could easily be separated and recovered from water using a magnet. This study thus identifies a promising and efficient technology for removing Cd(II) ions from aqueous solutions.

Keywords Carbon aerogels · Adsorption · Cd(II) · Magnetic nanoparticles

Introduction

Water pollution caused by heavy metal ions is of global concern and is implicated in a wide range of diseases (Ma et al. 2018; Sun et al. 2018; Zang et al. 2020). Cadmium ions are highly toxic (Kuang et al. 2019) and can enter drinking water source via a variety of pathways, including natural mineral weathering processes and also unlawful disposal of industrial waste water (Xu et al. 2018). Industrial sources of cadmium pollution include cooling tower sewage, metal electroplating solutions, and coating operations (Li et al. 2004). Ingested Cd(II) ions mainly accumulate in the kidneys and have a relatively long biological half-life of 10–35 years in the human body (Ammari 2014). The accumulation of Cd(II) ions in the body can lead to skin lesions, renal dysfunction, pneumonia, and cancer (Kuang et al. 2019).

Current technologies for treating water contaminated with cadmium ions include filtration (Xiong et al. 2017), liquid extraction (Al-Rashdi et al. 2013), biological treatment (Mahandra et al. 2017), chemical precipitation (Li et al. 2017), and membrane separation (Khosravi and Alamdari 2009). Each of these technologies has advantages and disadvantages, with most suffering from a low removal capacity, low removal rate, and high cost. The discovery of effective materials and methods for quickly removing Cd(II) ions from water at minimal cost is an urgent priority.

Adsorption-based methods are the widely used for removing Cd(II) from water (Sun et al. 2019). Adsorption methods are simple, offer good adsorption capacities, and create minimal secondary pollution (Yang et al. 2020). Current research focusses on modifying the adsorbent structure and

Responsible editor: Tito Roberto Cadaval Jr

Electronic supplementary material The online version of this article (https://doi.org/10.1007/s11356-020-10859-0) contains supplementary material, which is available to authorized users.

✉ Weijie Shi
swj1013@163.com

✉ Shiyun Ai
ashy@sdau.edu.cn

[1] College of Chemistry and Material Science, Shandong Agricultural University, 61 Daizong Street, Taian 271018, Shandong, People's Republic of China

[2] School of Chemical Sciences, The University of Auckland, Auckland 1142, New Zealand

[3] School of Environment and Materials Engineering, Yantai University, Yantai 264005, Shandong, People's Republic of China

morphology to improve the adsorbent surface area and surface functional groups, thus enhancing the adsorption capacity and reaction site density (Wang et al. 2018). Aerogels are attracting increasing interest in heavy metal adsorption, on account of their three-dimensional (3D) networks of interconnected pores. This architecture allows high water absorptivity and offers a large specific surface for adsorption (Liang et al. 2012; Ren et al. 2019). Xu et al. reported that a 3D titanate aerogel containing cellulose was an effective adsorbent for Cd(II) removal, achieving a Cd(II) adsorption capacity of 1.98 mmol g^{-1} (Xiong et al. 2017). He et al. (2016) synthesized sodium acrylate and acrylamide copolymer/graphene oxide gels which proved very effective for the adsorption of Pb^{2+} and Cd^{2+}. These studies demonstrate the huge potential of aerogels in the adsorption of heavy metals, though the synthesis of most current aerogels use toxic or expensive precursors or complex equipment which are a major obstacle to practical applications and commercialization. Synthetic routes must be discovered towards aerogels based on renewable biopolymers, thus allowing economical aerogel production on a large scale for heavy metal removal from water and other applications.

Sodium alginate (SA) is a natural polysaccharide which is comprised of α-l-guluronate (G) and β-d-mannuronate (M) units (Chen et al. 2013; Shalumon et al. 2011). Sodium alginate can be obtained from a wide range of sources, and as a by-product of algal processing is inexpensive. SA is rich in carboxyl groups (−COOH) and hydroxyl (−OH) groups (Chen et al. 2011). These functional groups play a key role in forming hydrogen bonds with water (thus giving SA unique gelling properties) and can also chelate metal ions (hence the property of alginates to form characteristic box structures in the presence of metal ions). Combining sodium alginate with other biopolymers offers the possibility of developing novel aerogel precursors. Gelatin (G) is a colloidal protein source obtained by boiling connective tissues found in animal skin, bone, and muscle membranes. Gelatin can be mixed with sodium alginate to form stiff gels, with the gelatin serving as a cross-linker of alginate chains (Alonso et al. 2019). Pyrolysis of such alginate-gelatin gels under a nitrogen atmosphere is expected to yield carbon aerogels rich in surface functional groups, such as –COOH and –OH moieties, making the carbon aerogels potentially very promising low cost adsorbents for Cd(II) and other heavy metals. Minimal work has been reported in this area to date, motivating a detailed investigation.

Carbon materials are widely used as absorbents, with the sorption properties of carbons easily tuned for specific applications via control of the pyrolysis temperature used in their synthesis (i.e., temperature and pyrolysis time control the degree of carbon graphitization, surface area, and the nature of the surface functional groups). In order to aid separation of carbon adsorbents from water and other media following adsorption of targeted ions or molecules, researchers are now seeking to develop magnetic adsorbent materials. This is typically achieved by incorporating nanoparticles of magnetite (Fe_3O_4) or a similar magnetic material into the adsorbent. This approach has been shown to allow rapid sorbent-liquid separations. Liu et al. (2012) successfully prepared a magnetic Fe_3O_4/chitosan hybrid hydrogel for the adsorption of heavy metals. Hu et al. (2018) synthesized an adsorbent composed of Fe_3O_4, chitosan and Al $(OH)_3$ using a solvothermal method, with the obtained adsorbent showing good properties for the adsorption of heavy metals. Thermal pyrolysis of Fe_3O_4-biopolymer gels under a N_2 atmosphere should afford novel magnetic Fe_3O_4@C aerogel sorbents for heavy metals, motivating a detailed investigation.

Herein, we develop a green and facile route to prepare a new magnetic carbon aerogel (MCA) containing Fe_3O_4 nanoparticles using sodium alginate as the carbon source. We first synthesized freeze-dried gels containing sodium alginate (SA), gelatin (G), and Fe_3O_4 nanoparticles, then heated the gels to 550 °C under N_2 to obtain magnetic carbon aerogels (MCAs). The MCAs were porous, hydrophilic (allowing easy dispersion in water), and magnetic (thus could be quickly separated from water using an external magnet), and were excellent adsorbents of aqueous Cd(II) (due to an abundance of surface -COOH and -OH groups). Compared with the other methods for aerogel preparation, our synthetic method offers many advantages including the following: (1) the synthesis of the MCAs uses only non-toxic, low cost reagents and (2) the pyrolysis step used to create the MCAs is simple and does not require expensive equipment. The very high adsorption capacity for Cd(II) offered by the MCAs validates the synthesis strategy introduced here.

Experimental

Materials and chemicals

Sodium alginate (99%) and gelatine (98%) were purchased from Aladdin Chemical Co. Ltd. (Shanghai, China). $FeCl_3.6H_2O$ (99%), ammonium hydroxide (30 wt%), $Cd(NO_3)_2$, and all other chemicals were of analytical grade and purchased from Sinopharm Chemical Reagent Company (Shanghai, China). All chemicals were used as received without further purification. Deionized water was used in all experiments.

Synthesis of carbonaceous gel and carbon aerogel

Gelatin (0.8 g) was added to 20 mL of water at 60 °C and stirred continuously (150–200 rpm) until a homogeneous solution was obtained. The stirring rate was reduced to 100 rpm, after which sodium alginate (SA, 2.0 g) was added to form a

viscous hydrogel (Saarai et al. 2013). The resulting SA/G hydrogel was then frozen in liquid N_2 and then freeze-dried. The carbonaceous gel (CG) obtained was then heated at 550 °C for 4 h (4 °C min^{-1}) in a nitrogen atmosphere to produce a carbon aerogel (CA).

Synthesis of magnetic carbon aerogel

Magnetic carbon aerogels containing Fe_3O_4 nanoparticles were prepared according to a literature method (Azizi et al. 2014). Firstly, gelatin (0.8 g) was dissolved in 20 mL water at 60 °C under continuous stirring (150–200 rpm), after which Fe_3O_4 nanoparticles (0.4 g) were added and the resulting dispersion ultrasonicated for 5 min. Subsequently, sodium alginate (2.0 g) was added to the dispersion under continuous stirring. The gel obtained was then frozen and placed in a freezer dryer for 1 day to obtain a Fe_3O_4/SA/G hydrogel. Subsequently, the Fe_3O_4/SA/G hydrogel was then heated at 550 °C for 4 h under flowing N_2 (4 °C min^{-1}). The product obtained was a magnetic carbon aerogel (MCA).

Materials characterization

The morphologies of the samples were examined by transmission electron microscopy (TEM, G2 F20, FEI Co., USA). The structure and chemical composition of samples were probed using X-ray diffraction (XRD, TTR-III X-ray diffractometer, Smartlab SE, Rigaku Co., Japan), Fourier transform infrared spectroscopy (FTIR, tensor II, BRUKER Co. Germany), and X-ray photoelectron spectroscopy (XPS, ESCALAB 250Xi, Thermo Co., USA). Magnetic properties of samples were investigated using a vibrating sample magnetometer (Bruker Co., Germany) with an applied field between − 20,000 and 20,000 Oe at room temperature. Brunauer-Emmett-Teller (BET) specific surface areas and Barrett, Joyner, and Halenda (BJH) pore size distributions of samples were obtained from N_2 adsorption/desorption isotherms collected at − 196 °C on automatic surface area and a pore analyzer (Gemini VII 2390 t, Micromeritics Co., Shanghai). Zeta potentials of samples dispersed in distilled water at ambient temperature were determined using a zetasizer 3000 (Malvern Co., USA).

Cd(II) adsorption experiments

Cd(II) adsorption studies were carried out at 293 K in polycarbonate tubes containing 60 mg L^{-1} Cd(II) solutions and 0.4 g L^{-1} MCA. The initial solution pH of the Cd(II) solution was adjusted using 0.1–0.01 mol/L NaOH or HCl solutions to allow the effect of pH on Cd(II) adsorption to be explored. Adsorption equilibrium was achieved in approximately 0.5 h at 293 K, with the MCA being easily separated from the solution using a magnet. The concentration of Cd(II) remaining in solution was determined at 228.8 nm in an atomic absorption spectrophotometer (Hitachi Z-2000, Japan). The detection limit was 0.005 mg/L; Cd(II) removal capacities q_e (mg/g) and removal efficiencies (%) were calculated as follows:

$$\text{Removal capacities } q_e = \frac{(c_0 - c_e)v}{m}$$

$$\text{Removal efficiency } (\%) = \frac{(c_0 - c_e)}{c_0} \times 100\%$$

where q_e is the equilibrium removal capacity (mg/g), c_0 and c_e are the initial and equilibrium Cd(II) concentrations (mg/L), respectively, V is the solution volume (mL), and m is the adsorbent mass (mg).

Results and discussion

Morphological and structural characterization of the magnetic carbon aerogel

Figure 1 shows TEM images of the carbonaceous gel (CG) and the magnetic carbon aerogel (MCA). The freeze-dried carbonaceous gel possessed a three-dimensional porous network structure with interconnection. This network structure is stiff owing to the cross-linking of alginate chains by gelatin. Figure 1b shows the porous structure of the CG precursor was retained following the pyrolysis step at 550 °C used in the synthesis of the MCA. The image shows a uniform distribution of Fe_3O_4 nanoparticles throughout the porous carbon network. The continuous porous structure of the MCA was expected to allow facile diffusion of Cd(II) to surface sites.

Powder XRD was applied to examine the structure of MCA (Fig. 2). The XRD pattern of MCA showed a multitude of diffraction peaks which are assigned as follows: The peak at $2\theta = 24.1°$ is assigned to the (003) reflection of graphitic carbon. Peaks around 34.72° and 62.08° correspond to the (311) and (440) planes of Fe_3O_4 (PDF card: #74-0748), respectively. The diffraction peaks at 42.68° and 48.21° correspond to the (211) and (131) planes of Fe_3C (PDF card: (#89-7271) (Gai et al. 2017), respectively. Peaks at 44.2° and 65.16° can be indexed to the (110) and (200) crystalline planes of Fe^0 (PDF card: #87-0722), respectively. These results suggest that during the pyrolysis step used in the synthesis of the MCA, a fraction of the Fe_3O_4 was reduced to Fe^0 and Fe_3C nanocrystals. The mechanism leading to the formation of these reduced iron species was likely as follows:

$$Fe_3O_4 + 4C \rightarrow 3Fe + 4CO\uparrow \quad (1)$$

$$3Fe + C \rightarrow Fe_3C \quad (2)$$

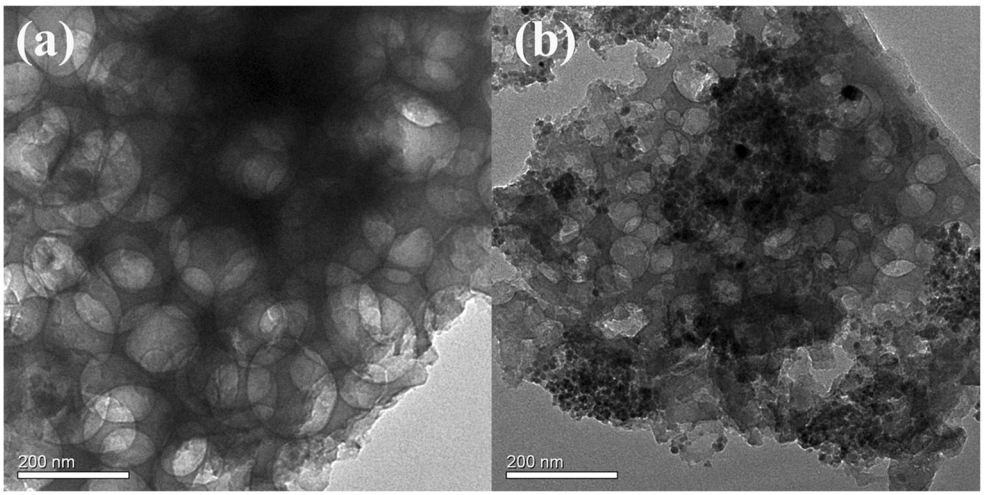

Fig. 1 TEM images of **a** CG and **b** MCA

Since the MCA still retained a significant Fe_3O_4 component, it was expected that the aerogel would still be magnetic, which was verified by the experiment below.

The Raman spectrum for MCA showed characteristic carbon D and G bands at 1356 and 1584 cm^{-1}, respectively (Fig. 2b). The intensity ratio of the D and G bands (I_D/I_G) was 0.98, implying that the carbon in the MCA had a reasonable degree of graphitization (Yao et al. 2017). The extent of graphitization of carbon materials controls the surface hydrophilicity/hydrophobicity. Highly graphitized carbons have high specific surface area but hydrophobic, which is undesirable for the removal of Cd(II) from water. The modest degree of

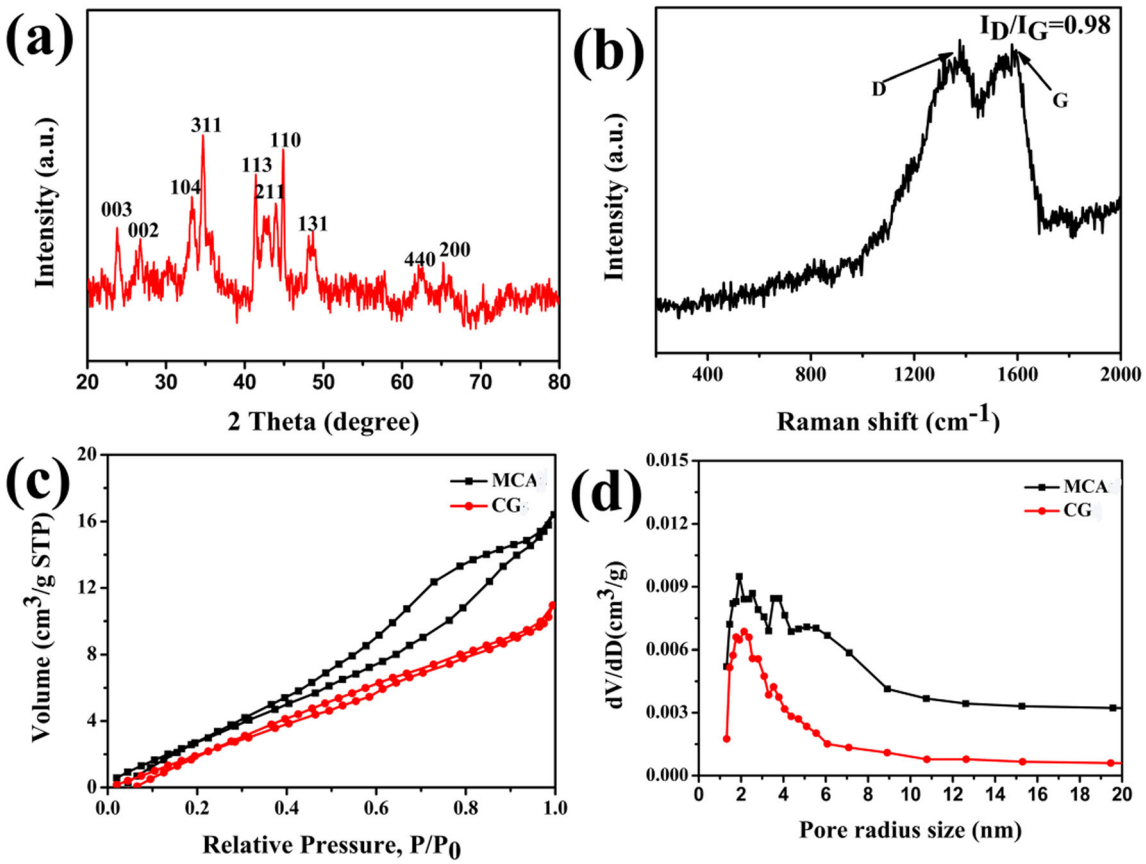

Fig. 2 **a** XRD pattern of MCA, **b** Raman spectrum of MCA, **c** N_2 adsorption and desorption isotherms, and **d** corresponding pore size distributions for CG and MCA

graphitization present in the MCAs was desirable, offering a high surface area but good hydrophilicity and thus water dispersibility (as explored below).

N_2 adsorption-desorption isotherms and BJH pore size distribution plots for both the CG and MCA are shown in Fig. 2c and d, respectively. BET specific surface areas determined from the N_2 physisorption isotherms of CG and MCA were 105.8 m^2/g and 145.7 m^2/g, respectively. The isotherms were consistent with a weak adsorbate-adsorbent interaction. Pore size distributions for CG and MCA showed pores with radii in the range 1–10 nm, indicating the presence of mesopores. The pore size range for MCA was slightly broader than that of CG, which is expected since the MCA was subjected to a pyrolysis treatment at 500 °C which was expected to open any existing pores. Since the TEM images for the CG and MCA samples showed the presence of numerous macropores (size > 100 nm), the CG and MCA samples can be considered hierarchically porous (i.e., contain pores of two quite distinct sizes).

Fourier transform infrared (FTIR) spectroscopy was used to examine the surface functional groups on the carbonaceous gel (CG) and the magnetic carbon aerogel (MCA). Results are shown in Fig. 3a. The spectra for CG and MCA were similar, containing many of the same peaks. The broad band at 3443 cm^{-1} is attributed to the O–H stretching vibrations of surface hydroxyl groups. The bands at 1128 and 864 cm^{-1} can be ascribed to the C–O stretching and C–OH bending deformations (Grzyb et al. 2010), respectively. The intense band at 1454 cm^{-1} arises from carboxylic O–H deformations or C–H bending vibration (Moreno-Castilla et al. 2000). A weaker feature is seen around 1650 cm^{-1} which is typical for asymmetric stretching vibrations of carboxylate species ($–CO_2^-$). Fe_3O_4 shows broad and intense bands ~ 625 cm^{-1} can readily be assigned to Fe–O stretching vibrations (Wang et al. 2013). This peak was weak in the spectrum of MCA due to the low Fe_3O_4 loading in the aerogel. To summarize, FTIR analysis revealed an abundance of hydroxyl, carbonyl, and carboxyl groups on the surface of the MCA. The presence of these groups was important to the functional properties of MCA, making the aerogel hydrophilic and providing binding sites for Cd(II).

The magnetization curve for MCA collected at room temperature is shown in Fig. 3b. The specific saturation magnetization (Ms) of MCA was 15.9 emu g^{-1}, consistent with the presence of superparamagnetic Fe_3O_4 nanoparticles embedded in a carbon matrix. The inset in Fig. 3b shows that the MCA powder could easily be lifted by a magnet, indicating that magnetic separation of the MCA from aqueous solution following Cd(II) adsorption should be readily achievable.

Adsorption kinetics

The kinetics of Cd(II) adsorption by MCA was first investigated using an initial Cd(II) concentration of 60 mg L^{-1}. Figure 4c shows that Cd(II) adsorption occurred rapidly during the first 20 min under continuous shaking, then increased slowly thereafter with adsorption equilibrium achieved after 1 h. The adsorption kinetics of Cd(II) was modeled using pseudo-first-order and pseudo-second-order adsorption models (Fig. 4e and f, respectively). The kinetic parameters and the correlation coefficients (R^2) were calculated from the linear regression applied to each plot. The pseudo-second-order model fitted the data extremely well, evidenced by the R^2 value of 0.999 (versus 0.930 for the pseudo-first-order model). On this basis, it can be concluded that the adsorption of Cd(II) on MCA obeys pseudo-second-order kinetics, typical for adsorption coupled with a chemical reaction process. An equilibrium adsorption capacity (q_e) of 143.88 mg/g was obtained from the pseudo-second-order model (in Table 1), very close to that determined from the adsorption data after 1 h (q_e = 143.15 mg/g).

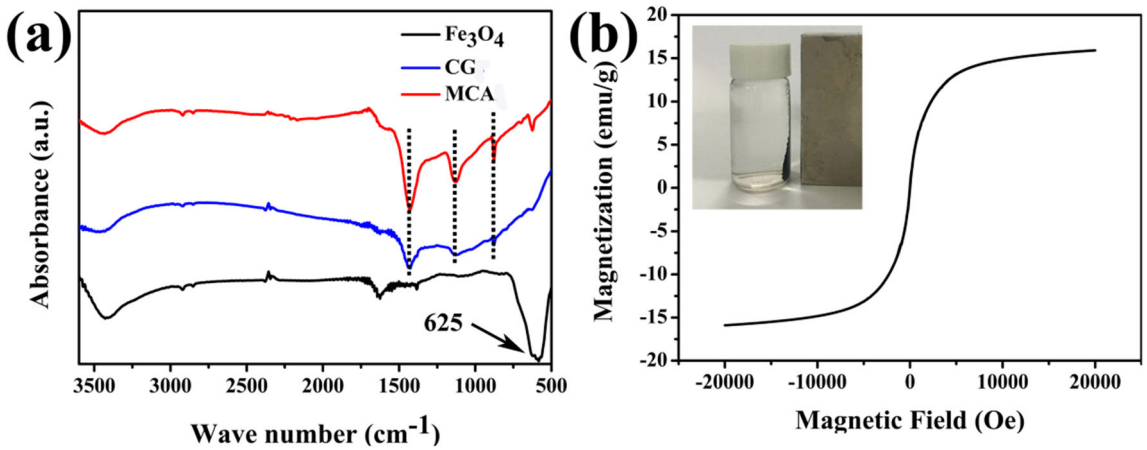

Fig. 3 **a** FTIR spectra for Fe_3O_4, CG, and MCA; **b** room temperature magnetic hysteresis loop for MCA. The inset in **b** shows the MCAs powder being lifted by a magnet

Table 1 Parameters obtained from different kinetic model

Model	Parameters		R^2
Pseudo-first-order	k_1 (min^{-1}) 0.0579	Q_e (mg g^{-1}) 4.9	0.931
Pseudo-second-order	k_2 (min^{-1}) 0.142	Q_e (mg g^{-1}) 143.88	0.999

Figure 4d examines the effect of pH on Cd(II) adsorption by MCA. The amount of Cd(II) adsorbed increased with solution pH, which was consistent with previous reports for Cd(II) adsorption on carbon adsorbents (Liu et al. 2020). The maximum Cd(II) removal capacity by MCA was 112.15 mg/g at pH 7, compared with only 69.74 mg/g at pH 1. In aqueous solutions of pH 1–7, Cd(II) ions are the dominant species in aqueous solution. At pH 1, the MCA surface will be positively charged and protonated (i.e., –OH, $–OH_2^+$ and –COOH will be the dominant surface functional groups). Accordingly, electrostatic attraction and binding of Cd(II) ions will be limited. As the pH increases, the MCA surface will be less protonated, with –OH, $–O^-$ and $–COO^-$ being the dominant surface functional groups on the MCA. Accordingly, positively charged Cd(II) ions will experience a stronger electrostatic attraction to the MCA surface, resulting in a higher removal capacity. Overall, the MCA showed a very high adsorption capacity for Cd(II) ions in the pH range 1–7, suggesting that the aerogel adsorbent offered good potential for Cd(II) removal from acidic or neutral wastewaters.

Figure 4a shows that the removal capacity of Cd(II) by both the carbonaceous gel (CG) and MCA was quite similar, increasing with the initial concentration of Cd(II). However, at low Cd(II) concentrations, the removal performance of MCAs was slightly superior relative to CG, which is likely due to the higher specific surface area of MCA compared with CG. When the cadmium ion concentration was 20 mg/L, the Cd(II) removal efficiency by MCA reached 98.7% (Fig. 4b), with a > 85% removal efficiency being achieved at concentrations up to 100 mg/L. MCAs thus offer great promise for Cd(II) removal from water. The US Environmental Protection Agency (EPA) has established a Maximum Contaminant Level (MCL) of 0.005 mg/L for drinking water. Assuming that the MCA can remove 99% of Cd(II) in 1 L of water at low concentrations, MCA would allow water with a Cd(II) concentration of 0.5 mg/L to be made safe for drinking in 1 h (requiring only 0.4 g of MCA to achieve this). Through successful treatments with fresh MCA, water with a much higher concentration of Cd(II) (e.g., 20 mg/L) could be made drinkable in only 1–2 h (with a MCA loading of 0.4 g/L each treatment).

The recyclability of MCA as an adsorbent for Cd(II) was studied. After Cd(II) adsorption in a 20 mg/L Cd(II) solution, the MCA was washed with an aqueous 0.1 mol/L HCl solution, then washed with water until the washing was neutral. As shown in Fig. S1, the Cd(II) removal efficiency decreased only slightly with repeated use, retaining 93% of the initial removal efficiency over 5 cycles. The results suggest that MCA had good stability and reusability, which are important properties in the development of a low cost and sustainable adsorbent.

Cd(II) removal mechanism

In order to obtain more detailed information about the mechanism of Cd(II) removal by MCA, zeta potential measurements, and pre and post Cd(II) adsorption analyses were performed on the magnetic carbon aerogel. Zeta potential data for MCA at different pH values are shown in Fig. 5a. The zeta potential of the MCA was positive at pH values between 1 and 3 and negative at pH values from 5 to 7. The results suggest that the isoelectric point for MCA is probably around 3.7–4.0. This explains why the adsorption capacity of MCA for Cd(II) ions increased with pH in the range 1–7, since above pH 4, the surface of MCA would be negatively charged and thus favor electrostatic binding of Cd(II).

Figure 5b shows that a FTIR peak appeared at 540 cm^{-1} following the Cd(II) adsorption experiment, which is assigned to a Cd–O stretching mode. The appearance of this feature coincided with an attenuation of the peaks at 864 and 1454 cm^{-1}, suggesting that Cd(II) removal involved complexation by surface –COOH and –OH groups of MCA.

Similar conclusions were obtained through XPS analysis. Figure 5c and d show C 1s and O 1s XPS spectra, respectively, for MCA before and after Cd(II) adsorption. The C 1s spectrum of the as-prepared MCA peaks (Fig. 5c) showed peaks at 284.7, ~ 285.5, and ~ 289.6 eV, which can readily be assigned to neutral hydrocarbons (i.e., C=C or C–C), and C–O and O=C–O carbon environments, respectively (Gollavelli et al. 2013). The O 1s spectrum of the as-prepared MCA contained an intense peak at 531.78 eV due to carboxyl O=C–O or C=O groups and a weaker peak at 535.82 eV assigned to surface –OH groups (Liu et al. 2013).

Following Cd(II) adsorption, some changes are seen in the C 1s and O 1s spectra. In the C 1s spectrum, the C 1s peak at 289.6 eV associated with O=C–O on the surface of MCA disappeared, and instead was replaced by a new C 1s peak at 288.2 eV. This shift to lower binding energies is explained by the complexation of Cd(II) by surface carboxylate groups of MCA, which reduced the electron withdrawing properties of the carboxyl oxygens (thus making the carboxyl carbon less positively charged). In the O 1s region, the O–H-related signal at 535.82 eV lost intensity after Cd(II) adsorption (Liu et al. 2013),

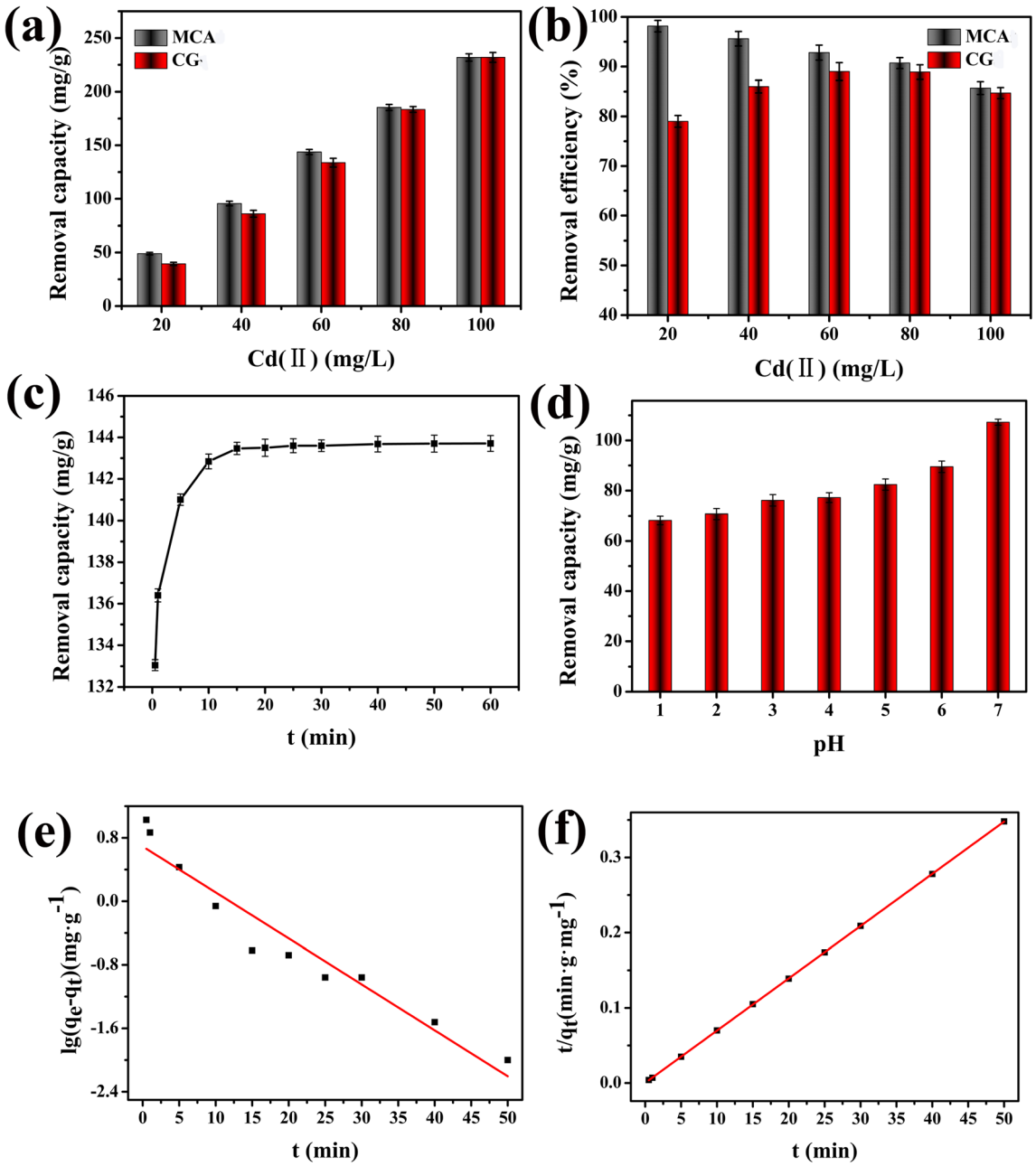

Fig. 4 **a** Effect of initial Cd(II) concentration on the removal capacity using CG and MCA as adsorbents (pH = 6.0 ± 0.1, adsorbent loading = 0.4 g/L, and adsorption time t = 60 min), **b** removal efficiency of Cd(II) by CG and MCA at different initial Cd(II) concentrations, **c** effects of contact time on the Cd(II) removal capacity by MCA (pH = 6.0 ± 0.1, MCA loading = 0.4 g/L, and c_o = 60 mg/L), and **d** effect of pH on Cd(II) removal capacity by MCAs (MCA loading = 0.4 g/L, c_o = 40 mg/L, and t = 60 min); **e** pseudo-first-order and **f** pseudo-second-order kinetic plots for Cd(II) removal by MCA (pH = 6.0 ± 0.1, m/V = 0.4 g/L, and c_o = 60 mg/L)

implying that Cd(II) also interacted with surface –OH groups of MCA (the resulting C–O–Cd moiety presumably has an O 1s binding energy similar to the carboxyl and carboxylate-Cd species). Combining the findings of the FTIR and XPS analyses, that oxygen-containing functional groups on the surface of MCA play a key role in the adsorption and removal of Cd(II) from water.

Based on the results and discussion above, a scheme for Cd(II) removal from water by MCA was developed, as shown in Fig. 5. Firstly, positively charged Cd(II) ions are adsorbed onto the porous carbon network of MCA by electrostatic attraction. Cd(II) ions are then strongly bound by complexation with surface carboxyl and hydroxyl groups of MCA. The magnetic properties of MCA (containing Fe_3O_4 nanoparticles) allow facile separation of MCA-Cd(II) from aqueous solution using a magnet, acid washing of MCA-Cd(II), followed by rinsing with water, regenerating MCA for reuse.

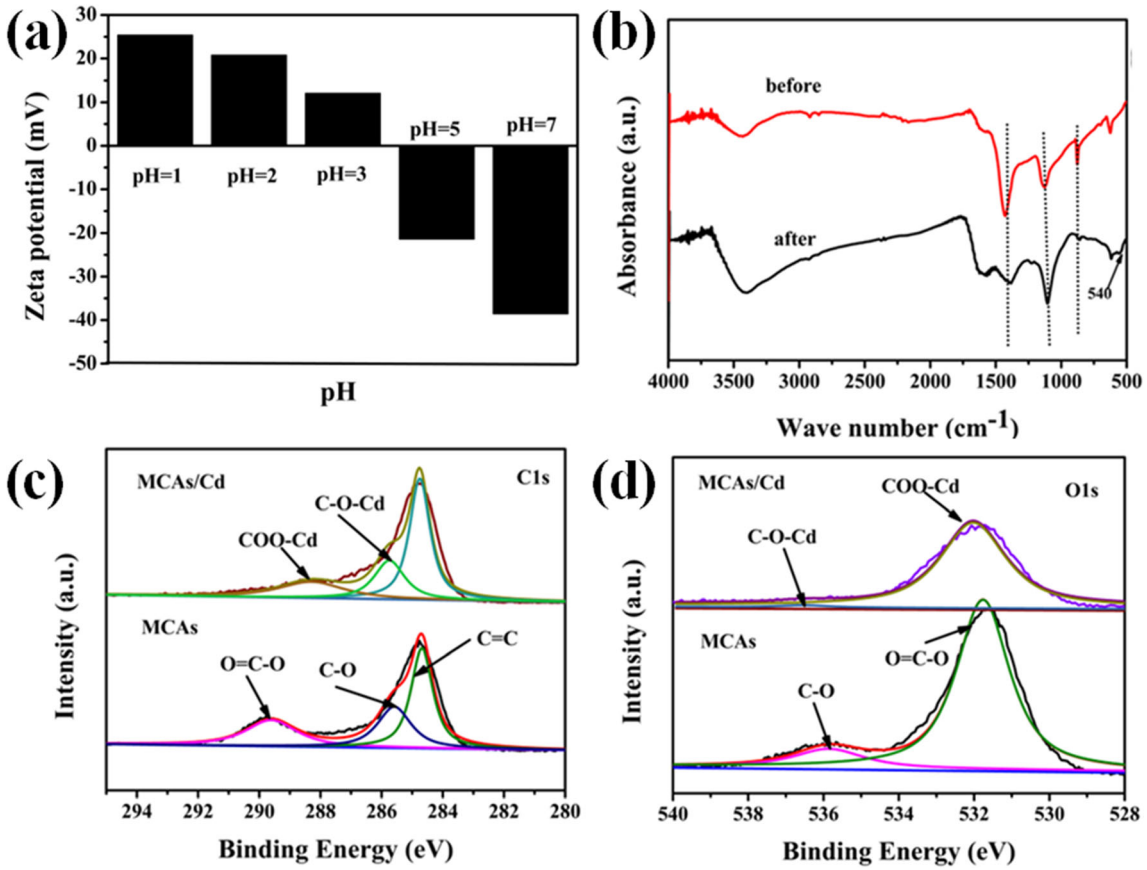

Fig. 5 **a** Zeta potential of MCA at different pH. **b** FTIR spectra for MCA before and after Cd(II) adsorption. XPS spectra for MCA before and after Cd(II) adsorption: **c** C 1s region and **d** O 1s region

Conclusions

In this study, we successfully developed a magnetic carbon aerogel (MCA) using sodium alginate and gelatin as the carbon source and Fe_3O_4 nanoparticles to impart magnetic properties. The MCA was rich in mesopores and macropores (surface area of 147 m^2 g^{-1}) and abundant in surface hydroxyl and carboxyl groups which allowed for easy dispersion in water. MCA offered outstanding performance for Cd(II) adsorption in water over the pH range 1–7, with the highest Cd(II) removal capacity found at pH 7. Cd(II) adsorption on MCA occurred through electrostatic attraction and complexation via surface carboxyl and hydroxyl groups. On account of the embedded Fe_3O_4 nanoparticles, the used MCA adsorbent could easily by separated from aqueous solution and regenerated via acid washing to release adsorbed Cd(II). The data presented suggests that the MCA developed in this study holds great promise as an adsorbent for removing Cd(II) from waste water and drinking water.

Acknowledgments The authors are thankful to the editor and the anonymous reviewers for their critical insightful comments and many constructive suggestions.

Authors' contributions Shiyun Ai and Weijie Shi contributed to the conception of the study. Mengqi Zhou performed the experiment. Jianchao Sun helped perform the analysis with constructive discussions. Geoffrey I.N. Waterhouse contributed significantly to analysis and manuscript preparation. Yingchao Li performed the experiment and was a major contributor in writing the manuscript. All authors read and approved the final manuscript.

Funding This work was supported by the National Natural Science Foundation of China (Nos. 41771342 and 41701350), the National Key R&D Program of China (2017YFD0801504), and the Natural Science Foundation of Shandong Province, China (No. ZR2017MD002). GINW acknowledges funding support from the MacDiarmid Institute for Advanced Materials and Nanotechnology.

Data availability All data generated or analyzed during this study are included in this published article (and its supplementary information files]).

Compliance with ethical standards

Competing interests The authors declare that they have no competing interests.

Ethics approval and consent to participate Not applicable.

Consent for publication Not applicable.

References

Alonso M, Enrique Guerrero-Beltrán C, Ortega-Lara W (2019) Design and characterization of gelatin/PVA hydrogels reinforced with ceramics for 3D printed prosthesis. Mater Today Proc 13:324–331

Al-Rashdi BAM, Johnson DJ, Hilal N (2013) Removal of heavy metal ions by nanofiltration. Desalination 315:2–17

Ammari TG (2014) Utilization of a natural ecosystem bio-waste; leaves of Arundo donax reed, as a raw material of low-cost eco-biosorbent for cadmium removal from aqueous phase. Ecol Eng 71:466–473

Azizi K, Karimi M, Nikbakht F, Heydari A (2014) Direct oxidative amidation of benzyl alcohols using EDTA@Cu(II) functionalized superparamagnetic nanoparticles. Appl Catal A Gen 482:336–343

Chen JH, Liu QL, Hu SR, Ni JC, He YS (2011) Adsorption mechanism of Cu(II) ions from aqueous solution by glutaraldehyde crosslinked humic acid-immobilized sodium alginate porous membrane adsorbent. Chem Eng J 173:511–519

Chen JH, Xing HT, Guo HX, Li GP, Weng W, Hu SR (2013) Preparation, characterization and adsorption properties of a novel 3-aminopropyltriethoxysilane functionalized sodium alginate porous membrane adsorbent for Cr(III) ions. J Hazard Mater 248-249:285–294

Gai C, Zhang F, Lang Q, Liu T, Peng N, Liu Z (2017) Facile one-pot synthesis of iron nanoparticles immobilized into the porous hydrochar for catalytic decomposition of phenol. Appl Catal B Environ 204:566–576

Gollavelli G, Chang C-C, Ling Y-C (2013) Facile synthesis of smart magnetic graphene for safe drinking water: heavy metal removal and disinfection control. ACS Sustain Chem Eng 1:462–472

Grzyb B, Hildenbrand C, Berthon-Fabry S, Bégin D, Job N, Rigacci A, Achard P (2010) Functionalisation and chemical characterisation of cellulose-derived carbon aerogels. Carbon 48:2297–2307

He S, Zhang F, Cheng S, Wang W (2016) Synthesis of sodium acrylate and acrylamide copolymer/GO hydrogels and their effective adsorption for Pb2+ and Cd2+. ACS Sustain Chem Eng 4:3948–3959

Hu H, Yang L, Lin Z, Xiang X, Jiang X, Hou L (2018) Preparation and characterization of novel magnetic Fe3O4/chitosan/Al(OH)3 beads and its adsorption for fluoride. Int J Biol Macromol 114:256–262

Khosravi J, Alamdari A (2009) Copper removal from oil-field brine by coprecipitation. J Hazard Mater 166:695–700

Kuang M, Shang Y, Yang G, Liu B, Yang B (2019) Facile synthesis of hollow mesoporous MgO spheres via spray-drying with improved adsorption capacity for Pb(II) and Cd(II). Environ Sci Pollut Res 26: 18825–18833

Li Q, Wu S, Liu G, Liao X, Deng X, Sun D, Hu Y, Huang Y (2004) Simultaneous biosorption of cadmium (II) and lead (II) ions by pretreated biomass of Phanerochaete chrysosporium. Sep Purif Technol 34:135–142

Li X, Dai L, Zhang C, Zeng G, Liu Y, Zhou C, Xu W, Wu Y, Tang X, Liu W, Lan S (2017) Enhanced biological stabilization of heavy metals in sediment using immobilized sulfate reducing bacteria beads with inner cohesive nutrient. J Hazard Mater 324:340–347

Liang H-W, Guan Q-F, Chen L-F, Zhu Z, Zhang W-J, Yu S-H (2012) Macroscopic-scale template synthesis of robust carbonaceous nanofiber hydrogels and aerogels and their applications. Angew Chem Int Ed 51:5101–5105

Liu Z, Wang H, Liu C, Jiang Y, Yu G, Mu X, Wang X (2012) Magnetic cellulose–chitosan hydrogels prepared from ionic liquids as reusable adsorbent for removal of heavy metal ions. Chem Commun 48: 7350–7352

Liu H, Gao Q, Dai P, Zhang J, Zhang C, Bao N (2013) Preparation and characterization of activated carbon from lotus stalk with guanidine phosphate activation: sorption of Cd(II). J Anal Appl Pyrolysis 102: 7–15

Liu J, Huang Z, Sun J, Zou Y, Gong B (2020) Enhancing the removal performance of Cd(II) from aqueous solutions by NaA zeolite through doped thiourea reduced GO which is trapped within zeolite crystals. J Alloys Compd 815:152514

Ma Q, Cui L, Zhou S, Li Y, Shi W, Ai S (2018) Iron nanoparticles in situ encapsulated in lignin-derived hydrochar as an effective catalyst for phenol removal. Environ Sci Pollut Res 25:20833–20840

Mahandra H, Singh R, Gupta B (2017) Liquid-liquid extraction studies on Zn(II) and Cd(II) using phosphonium ionic liquid (Cyphos IL 104) and recovery of zinc from zinc plating mud. Sep Purif Technol 177:281–292

Moreno-Castilla C, López-Ramón MV, Carrasco-Marín F (2000) Changes in surface chemistry of activated carbons by wet oxidation. Carbon 38:1995–2001

Ren B, Wang K, Zhang B, Li H, Niu Y, Chen H, Yang Z, Li X, Zhang H (2019) Adsorption behavior of PAMAM dendrimers functionalized silica for Cd(II) from aqueous solution: experimental and theoretical calculation. J Taiwan Inst Chem Eng 101:80–91

Saarai A, Kasparkova V, Sedlacek T, Saha P (2013) On the development and characterisation of crosslinked sodium alginate/gelatine hydrogels. J Mech Behav Biomed Mater 18:152–166

Shalumon KT, Anulekha KH, Nair SV, Nair SV, Chennazhi KP, Jayakumar R (2011) Sodium alginate/poly(vinyl alcohol)/nano ZnO composite nanofibers for antibacterial wound dressings. Int J Biol Macromol 49:247–254

Sun X, Zhu J, Gu Q, You Y (2018) Surface-modified chitin by TEMPO-mediated oxidation and adsorption of Cd(II). Colloids Surf A Physicochem Eng Asp 555:103–110

Sun C, Chen T, Huang Q, Wang J, Lu S, Yan J (2019) Enhanced adsorption for Pb(II) and Cd(II) of magnetic rice husk biochar by KMnO4 modification. Environ Sci Pollut Res 26:8902–8913

Wang T, Zhang L, Wang H, Yang W, Fu Y, Zhou W, Yu W, Xiang K, Su Z, Dai S, Chai L (2013) Controllable synthesis of hierarchical porous Fe3O4 particles mediated by poly(diallyldimethylammonium chloride) and their application in arsenic removal. ACS Appl Mater Interfaces 5:12449–12459

Wang W, Liu Y, Liu X, Deng B, Lu S, Zhang Y, Bi B, Ren Z (2018) Equilibrium adsorption study of the adsorptive removal of Cd2+ and Cr6+ using activated carbon. Environ Sci Pollut Res 25:25538–25550

Xiong Y, Wang C, Wang H, Yao Q, Fan B, Chen Y, Sun Q, Jin C, Xu X (2017) A 3D titanate aerogel with cellulose as the adsorption-aggregator for highly efficient water purification. J Mater Chem A 5:5813–5819

Xu J, Cao Z, Zhang Y, Yuan Z, Lou Z, Xu X, Wang X (2018) A review of functionalized carbon nanotubes and graphene for heavy metal adsorption from water: preparation, application, and mechanism. Chemosphere 195:351–364

Yang Z, Chen X, Li S, Ma W, Li Y, He Z, Hu H, Wang T (2020) Effective removal of Cd(II) from aqueous solution based on multifunctional nanoporous silicon derived from solar kerf loss waste. J Hazard Mater 385:121522

Yao Y, Lian C, Wu G, Hu Y, Wei F, Yu M, Wang S (2017) Synthesis of "sea urchin"-like carbon nanotubes/porous carbon superstructures derived from waste biomass for treatment of various contaminants. Appl Catal B Environ 219:563–571

Zang T, Wang H, Liu Y, Dai L, Zhou S, Ai S (2020) Fe-doped biochar derived from waste sludge for degradation of rhodamine B via enhancing activation of peroxymonosulfate. Chemosphere 261: 127616